Computers and Geotechnics 99 (2018) 191–202

Contents lists available at ScienceDirect

Computers and Geotechnics

journal homepage: www.elsevier.com/locate/compgeo

Research Paper

Modelling the mechanical behaviour of a natural unsaturated pyroclastic soil within Generalized Plasticity framework

Sabatino Cuomo[a,*], Mariagiovanna Moscariello[a], Diego Manzanal[b,c], Manuel Pastor[b], Vito Foresta[a]

[a] University of Salerno, Lab. Geotechnics, Department of Civil Engineering, Via Giovanni Paolo II, 132, 84084 Fisciano, SA, Italy
[b] Universidad Politécnica de Madrid, Department of Applied Mathematics and Computer Science, ETS Ingenieros de Caminos, UPM Madrid, Spain
[c] INTECIN, UBA, UNPSJB, CONICET, Argentina

ARTICLE INFO

Keywords:
Volcanic soil
Unsaturated
Collapse
Liquefaction
Constitutive model

ABSTRACT

The paper deals with the mechanical behaviour of a natural volcanic silty soil sampled from steep slopes. This soil is very loose and unsaturated over most of the year due to climate conditions. Thus so-called wetting collapse and static liquefaction may occur during rainfall. Major issues are posed once the slides turn into flows with high destructive potential. However, the modelling of the constitutive behaviour is challenging and not yet available in the literature for this soil. A recent Generalized Plasticity Model was selected as it is capable to adequately take into account the effects of change in soil porosity, bonding related to the matric suction normalized versus soil porosity, and static liquefaction proneness. The model is calibrated for 37 saturated/unsaturated laboratory tests, and the performance of the model is assessed quantitatively. It is newly shown that the model – with one single set of constitutive parameters – is capable to well describe the soil mechanical response, in unsaturated and saturated conditions, experienced by the soil in different laboratory devices and along different stress paths. Those insights provide a theoretical framework for designing further laboratory tests, improving the understanding of this complex natural soil, and implementing better modelling of landslides of the flow-type.

1. Introduction

Natural volcanic air-fall soils show peculiar features, as well documented in recent literature [2,9,7,46,16]. Two specific mechanical responses are typical of those soils: (i) “static liquefaction” in saturated condition for undrained shearing, and (ii) so-called “volumetric collapse” in unsaturated conditions upon wetting.

Static liquefaction is typical of loose saturated sands [24,56,11] but similar behaviour was later observed also for silty sands or sandy silts [50,39]. More recent discussions pointed out that strain localisation is more important under plane-strain or 3D conditions compared to triaxial conditions [53,54]. These insights also underline that soil behaviour should be extensively investigated along different stress paths, and possibly for different conditions, e.g. saturated or partially saturated condition.

For unsaturated soil, the wetting-induced collapse consists in a decrease of total volume of a soil due to wetting at essentially unchanged total vertical stress. The occurrence and the magnitude of the collapse depends on several factors: (i) an open, potentially unstable soil structure [59]; (ii) a net total stress high enough to make the structure metastable; (iii) a bonding or cementing agent that stabilizes the soil in unsaturated condition [42]. Aimed to investigate this topic, Jennings and Knight [22] firstly proposed the “double oedometer” method, based on standard oedometer tests at natural water and saturation. However, no information related was achievable for the influence of wetting-drying cycles, later investigated for lightly compacted soils of Hong Kong [10] and compacted specimens of clay subjected to wetting-drying cycles soon after moulding [47]. The effect of triaxial state stress on the collapse occurrence was more recently investigated on collapsible lower Cromer till [1], poorly compacted sandy clay [26], compacted kaolin [55], powder clay [23] and clayey sand [52]. The quantitative simulation of the soil mechanical response requires the use of advanced constitutive models, capable to deal with the hydro-mechanical coupling in both saturated and unsaturated conditions. Several constitutive equations or models have been proposed to predict the behaviour of unsaturated soils. A fundamental contribution was provided by Alonso et al. [1], who proposed the so-called Basic Barcelona Model (BBM). In this model, the Critical State Theory [44] joined to the Classic Plasticity [21] is extended to unsaturated soils. BBM has been used so far to simulate the mechanical behaviour of moderate expansive

* Corresponding author.
E-mail address: scuomo@unisa.it (S. Cuomo).

https://doi.org/10.1016/j.compgeo.2018.03.006
Received 21 July 2017; Received in revised form 30 January 2018; Accepted 12 March 2018

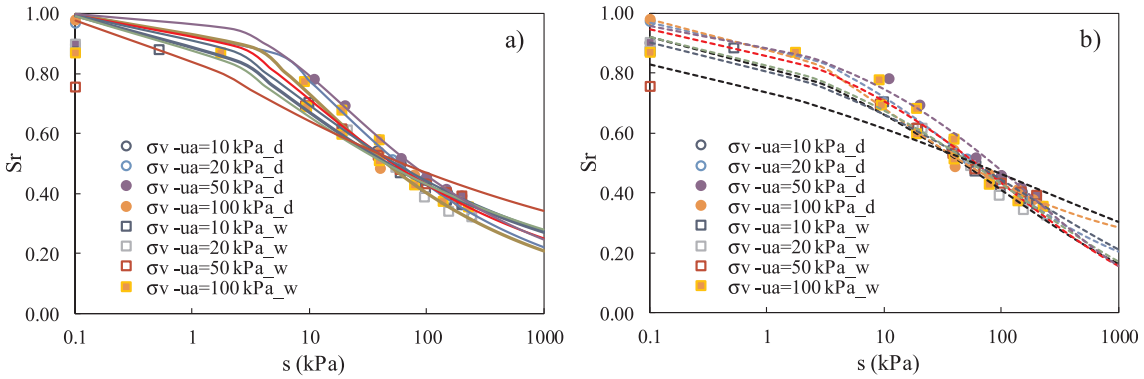

Fig. 1. Soil Water Retention Curve (SWRC) for different net vertical stress (σ_v-u_a) obtained through suction-controlled oedometer tests and interpolated through Van Genuchten model (a) and Fredlund and Xing model (b).

soils (like sands, silts, clayey sands, sandy clays or clays with a low plasticity). The stress variables of the BBM are the matric suction, the net stress (difference of total stress to the air pressure) and the specific volume, which is used as a state parameter. The model is capable to simulate: (i) the collapse or swelling, at different stress levels, due to a reduction of suction at constant net stress; (ii) the yielding of the soil due to the change of suction or net stress; (iii) the increase of the cohesion intercept due to an increase of suction. It is also worth mentioning the contributions of Wheeler and Sivakumar [55], who formulated an elasto-plastic-hardening model, starting from BBM model. An alternative approach is based on the Generalized Plasticity Theory [41,48,31], which will be used later on.

Notwithstanding the availability of comprehensive models, the mechanical behaviour of unsaturated volcanic air-fall soils is still limitedly addressed mostly because of the absence of extensive data-set of laboratory results. Other significant open issues are related to user-independent model calibration and quantitative assessment of model performance for complex constitutive models including many parameters.

The paper tries to fill this gap in the scientific literature modelling the mechanical behaviour of a complex natural soil: (i) in a wide range of states, from partially- to fully-saturated, in drained or undrained condition, and along different stress paths and confinement constraints including oedometric and triaxial; and (ii) using a comprehensive data-set. Thus, the paper provides an application of a model selected from the literature as it is capable to well reproduce important features of soil mechanical response. A procedure for model calibration is here proposed, and a systematic assessment of model performance is presented using a new-defined error function applicable also to other constitutive models.

The paper is organized as follows. It firstly presents the main peculiarities of a natural (air-fall volcanic) pyroclastic soil of Southern Italy, often involved in catastrophic landslides of the flow type [8,9,7], and the experimental laboratory testing programme developed in saturated and unsaturated soil conditions. Then, the Modified Pastor - Zienkiewicz constitutive model is presented [40,32,33], based on the fundamental concept of state and bonding parameter, which allows to accurately describing wide range of densities, confining pressure and suctions within a unitary framework, and through a unique set of constitutive parameters. Finally, calibration and performance of the constitutive model are discussed.

2. A vesuvian pyroclastic soil

The paper deals with an unsaturated air-fall volcanic (pyroclastic) soil of Southern Italy, originated from the explosive activity of the Somma-Vesuvius volcanic apparatus [8]. It is worth of note that: (i) the soil investigated resembles the behaviour of similar air-fall volcanic soils widespread all over the world (in almost 1% of Earth surface, [12], (ii) those soils are frequently involved in catastrophic landslides, (iii) there is still a lack of contributions regarding a comprehensive modelling of constitutive behaviour of such soils.

The soil investigated, classifiable as “class A” ashy soil according to Bilotta et al. [2], was involved in huge flow-like landslides occurred in May 1998, which caused many victims and damaged four towns at the toe of Pizzo d’Alvano massif. Since that time, slope failure and landslide propagation have been extensively studied [8,60]; among many others), while the soil constitutive behaviour has been oversimplified, as rigid perfectly-plastic, e.g. Cascini et al. [8], or elastic perfectly-plastic, e.g. Cascini et al. [9]. Whereas, more sophisticated and realistic constitutive models have been already used for other types of soils well reproducing slope failure, soil liquefaction and transformation from slide to flow (e.g. [7].

The soil grain size distribution consists in 43.6 to 51.9% Sand, 43.9 to 54.0% Silt, 1.4 to 4.7% Clay; soil specific gravity (G_s) is equal to 2.55; void ratio (e) ranges from 2.595 (undisturbed) to 1.982 (remoulded); the saturation degree (S_r) is comprised between 74.8% (undisturbed) and 92.1% (remoulded); the dry unit weight (γ_d) is 6.93 kN/m^3 to 8.65 kN/m^3 (respectively, undisturbed and remoulded). The average water content (w) is 51.9%, while the liquid limit (w_L) is 53.8% and the plastic limit (w_P) is 49.3% [3]. Due to the voids internal to the solid particles, this soil has a high porosity (0.53–0.74) and low soil unit weight (8.88–14.40 kN/m^3). Most of the studies investigated the role of matric suction, which is lowered by rainfall with dramatic consequences for slope stability. Thus, it is useful drawing some basic mechanical features.

The Soil Water Retention Curve (SWRC), relating the degree of saturation (S_r) to the matric suction (s), was obtained from drying and wetting tests (labelled as “d” and “w”, respectively in Fig. 1) conducted in Suction Controlled Oedometer tests [2,45] on undisturbed specimens at three different total net stresses (σ_v-u_a) equal to 10, 20 and 50 kPa. The experimental results (Fig. 1) show for SWRC a moderate variability, which is related to the inner nature of the air-fall soil under investigation. However, each experimental curve is well interpreted by Van Genuchten [51] model (with parameters: α equal to 0.19–1.02, n equal to 1.19–1.79, and m equal to 0.16–0.44) and Fredlund and Xing [18] model (with parameters: α equal to 23.59–448.38, m equal to 2.60–16.15 and n equal to 0.31–0.72):

$$S_r = S_{r0} + (1-S_{r0})\left[\frac{1}{1+(a\cdot s)^n}\right]^m \quad (1)$$

$$S_r = S_{r0} + (1-S_{r0})\left\{\frac{1}{\ln[e+(a\cdot s)^n]}\right\}^m \quad (2)$$

where S_{r0} is the residual saturation degree, s is the matric suction equal to u_a - u_w, u_a is the pore air pressure, u_w is the pore water pressure, a, m and n are parameters of the models, e is Euler's number.

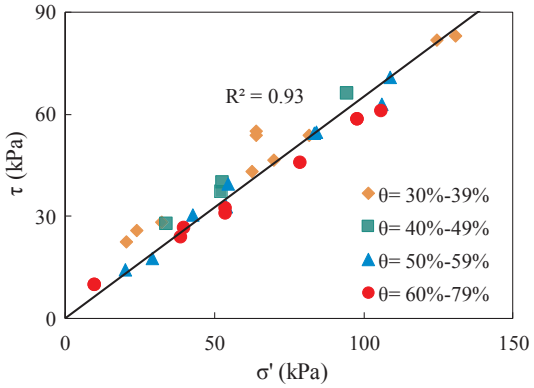

Fig. 2. Shear strength envelope of Standard Direct Shear stress performed at different volumetric water content (θ).

While both the models cannot account for dependence on void ratio and hydraulic hysteresis, that feature could be reproduced by the constitutive model applied later. The dependence of shear strength on suction was well outlined by Suction Controlled Direct Shear Tests [2,25,36,3] and standard Direct shear stress performed at natural water content [46]. The soil behaviour in both saturated and unsaturated condition was addressed through the effective stress tensor formulated as proposed by Bishop [4], in terms of relative degree of saturation (S_{re}) as follows:

$$\boldsymbol{\sigma}'_{ij} = \boldsymbol{\sigma}_{ij} - u_a \cdot \boldsymbol{\delta}_{ij} + S_{re} \cdot (u_a - u_w) \cdot \boldsymbol{\delta}_{ij} \quad (3)$$

where $\boldsymbol{\sigma}_{ij}$ is the total stress tensor, $S_{re} = (S_r - S_{ro})/(1 - S_{r0})$ is the "effective saturation degree", S_r is the current saturation degree, and $\boldsymbol{\delta}_{ij}$ is the Kronecker delta. In the triaxial plane, the Bishop equation is equal to:

$$p' = (p - u_a) + S_{re} \cdot s \quad (4)$$

where p is the total isotropic stress, and $p\text{-}u_a$ is referred as net isotropic stress.Fig. 2 shows the shear strength at failure versus the normal effective stress defined as for Eq. (3). The friction angle is about 30.1° to 34.8°, while cohesion intercept is about 5 kPa.

This paper is based on the results of a significant amount (37) of laboratory tests, partly used for calibration and partly used to assess the performance of the constitutive model. All of the tests were carried out on undisturbed specimens, sampled in the area of Sarno (N 40°50′28.71″, E 14°37′07.10″) - one of the villages located at the toe of the Pizzo d'Alvano massif -. The main experimental results are hereafter briefly described, while the specific experimental results will be shown in the next sections and compared to the fitting (calibration) or prediction (performance) of the constitutive model. Standard compression triaxial tests (Table 1) were performed, in drained or undrained condition, on undisturbed saturated specimens [36]. Particularly, three Consolidated Isotropically Drained (CID) compression triaxial tests were performed with initial void ratio (e) from 2.01 to 2.28 to individuate stiffness and shear strength of the soil and volumetric behaviour at failure. Three Consolidated Isotropically Undrained (CIU) compression triaxial tests were performed on specimens with initial void ratio (e) from 2.07 to 2.19, to quantify the occurrence of static liquefaction and the build-up of pore pressure over such unstable mechanical response. Suction-Controlled Triaxial (SCTX) tests were performed on specimen with initial void ratio ranges between 1.94 and 2.12, at suction (s) of 10, 20 and 50 kPa and at three net isotropic stress after consolidation $(p\text{-}u_a)_{cons}$, equal to 10, 30 and 50 kPa (Table 2). This group of tests was useful to assess the role of matric suction towards the increase of: (i) stiffness, and (ii) shear strength. Soil collapsibility was investigated through different devices: standard oedometer, suction-controlled oedometer and triaxial apparatus (Table 3). In particular, the wetting tests in standard oedometer (ED) were performed on specimens at natural water content corresponding to an initial suction of about 50 kPa, while the suction-controlled oedometer (SCED) and the suction-controlled wetting triaxial (ISO or Triaxial) tests were also performed starting from initial suction of 50 kPa. Doing so, the investigated stress paths were oedometric (k_0), isotropic ($\eta = 0$) and triaxial ($0.73 < \eta < 1$), while the suction was reduced by two different procedures: (i) suddenly flooding the specimen with distilled water at the top (tests type: ED), or (ii) gradually increasing the pore water pressure at the bottom of the specimens (test type: SCED, Triaxial and ISO). The experimental results outline that the magnitude of soil collapse is strongly influenced by: i) initial void ratio, ii) vertical net stress before wetting and iii) type of test (Fig. 3).

Table 1
Triaxial tests on saturated specimens.

Test	*Type*[a]	p'_{cons}	e_0	D_r
BIS02_05	CID	50	2.281	0.27
BIS13_04	CID	100	2.11	0.34
BIS05_05	CID	150	2.007	0.39
BIS01_05	CIU	50	2.188	0.31
BIS03_05	CIU	100	2.113	0.35
BIS06_05	CIU	150	2.065	0.37
BIS09_04	CID	50	2.385	0.22
BIS04_05	CID	100	2.059	0.37
BIS08_04	CID	150	2.282	0.36
BIS07_05	CIU	50	2.338	0.24

p'_{cons} = mean effective stress after consolidation stage; e_0 = initial void ratio; D_r = initial relative density
[a] CID = Consolidated Isotropically Drained, CIU = Consolidated Isotropically Undrained.

3. Constitutive model

The simulation of such complex mechanical behaviour required the use of an advanced constitutive model, i.e. Modified Pastor Zienkiewicz (MPZ) model recently proposed by Pastor et al. [40] and Manzanal et al. [32], Manzanal et al. [33].

The model selected refers to the Generalized Plasticity Theory introduced by Pastor and Zienkiewicz [41], which is particularly suitable to describe the behaviour of either loose or dense granular soils, both in drained and undrained conditions, even along complex stress paths. The original (Pastor Zienkiewicz) PZ model was fully defined through: (i) the elastic constitutive tensor; (ii) the unit tensor discriminating loading and unloading conditions. (iii) the unit tensor describing the direction of plastic flow in loading and unloading and (iv) the loading and unloading plastic moduli. The PZ model was also implemented in the FEM code named "GeHoMadrid" [17], and applied to rainfall and wetting-induced failure in partially saturated real slopes and flume tests (e.g. [17,7]. The MPZ model extended the original formulation to: (i) a unified approach to reproduce granular materials behaviour for a wide range of confining pressures and densities (or void ratios) with a single set of constitutive parameters [31,32], (ii) soil unsaturated condition [40,33] and (iii) crushable granular soils [34]. The MPZ model has been implemented "GeHoMadrid" FEM code in order to reproduce real boundary value problems such as harbour performance in a loose seabed [37,38].

The main features of the model are briefly recalled, while the details can be found in the references listed above. The MPZ model is based on the concept of a generalized state parameter for unsaturated state, two pairs of stress–strain variables and a suitable hardening law taking into account the bonding-debonding effect of suction and degree of saturation. The state parameter (ψ) represents the relationship between void ratio (relative density) and confining pressure. In other words, the state parameter describes (in e-p' plane) the current state in relation to its projection on the Critical State Line (CSL). If the state parameter is positive the sand presents a loose nature and soil behaviour is

Table 2
Triaxial tests on unsaturated specimens.

Test	Stress Path[a]	e_0 –	e_{cons} –	s (kPa)	$(p\text{-}u_a)_{max}$ (kPa)	$(p\text{-}u_a)_{cons}$ (kPa)	$S_{r\ ini}$ –	$S_{r\ cons}$ –
USP04_04	ISO	2.474	–	10	430	–	0.738	–
USP06_04	ISO	2.239	–	20	600	–	0.746	–
USP07_04	ISO	2.381	–	20	510	–	0.712	–
USP02_06	ISO	2.244	–	50	520	–	0.647	–
USP03_06	ISO	2.184	–	50	475	–	0.613	–
USP01_07	ISO	2.341	–	50	305	–	0.583	–
USP01_02	SCTX	2.314	2.001	50	–	50	–	0.616
USP03_02	SCTX	2.095	2.082	50	–	10	–	0.564
USP01_03a	SCTX	2.497	–	50	–	–	–	0.615
USP01_03b	SCTX	–	–	50	–	–	–	–
USP01_03c	SCTX	–	–	50	–	–	–	–
USP12_02	SCTX	2.460	2.410	10	–	50	–	0.705
USP15_02	SCTX	2.236	2.122	10	–	50	–	0.717
USP01_04	SCTX	2.393	2.328	10	–	10	–	0.835
USP02_04	SCTX	2.274	2.217	10	–	30	–	0.758
USP05_02	SCTX	2.032	1.940	20	–	50	–	0.612
USP05_04	SCTX	2.523	2.407	20	–	10	–	0.683
USP06_06	ISO	2.239	–	20	600	–	0.746	–
USP02_06	ISO	2.244	–	50	520	–	0.647	–
USP03_06	ISO	2.184	–	50	475	–	0.613	–
USP01_07	ISO	2.341	–	50	305	–	0.583	–
USP01_02	SCTX	2.314	2.001	50	–	50	–	0.616
USP03_02	SCTX	2.095	2.082	50	–	10	–	0.564
USP05_04	SCTX	2.319	2.288	50	–	30	–	0.557

[a] ISO = isotropic compression, SCTX = suction-controlled triaxial tests; e_0 = initial void ratio; e_{cons} = void ratio at consolidation stage; s = suction; $(p\text{-}u_a)_{max}$ = maximum net total isotropic stress reached upon Isotropic compression; $(p\text{-}u_a)_{cons}$ = net total isotropic stress after consolidation stage; $S_{r\ ini}$ = initial degree of saturation; $S_{r\ cons}$ = degree of saturation after consolidation stage.

Table 3
Wetting tests on unsaturated specimens lowering suction (u_a-u_w) from 50 kPa to zero, under constant net vertical stress (σ_v–u_a).

Test type[a]	Test	e_0	e_w	$\sigma_v - u_a$ (kPa)
SCED	ESA13_03	2.537	2.2295	95
	ESA9_03	1.992	1.860	295
	ESA10_04	1.902	1.827	500
ISO	USP6_06	2.217	2.167	100
	USP1_07	1.889	1.830	311
	USP3_06	1.762	1.734	477
ED	ESL7_03	2.513	2.245	95
	ESL9_03	2.245	2.053	297
	ESL11_03	1.881	1.765	594

[a] SCED = wetting test performed through suction-controlled oedometer; ISO = wetting tests performed in isotropic condition; ED = wetting test performed through standard oedometer; e_0 initial void ratio; e_w void ratio after wetting; $(\sigma_v - u_a)$ net vertical stress; ε_v volumetric strain after wetting.

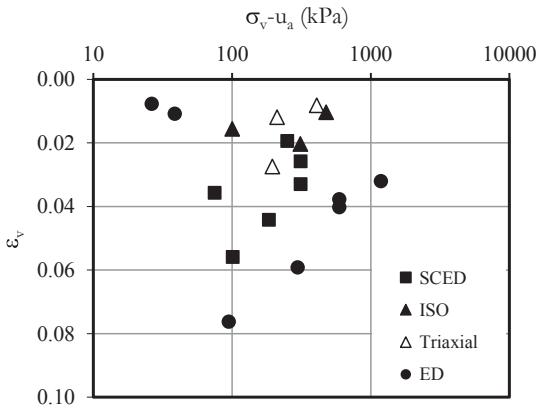

Fig. 3. Volumetric deformations versus net vertical stress (σ_v-u_a) measured through wetting tests in different devices (SCED: Suction Controlled Oedometer, ISO: isotropic conditions, TX: Triaxial condition, ED: standard oedometer).

contractive, otherwise the soil presents a dense nature and soil is dilatant. The loose or dense nature of the sand depends on the joint effect of its density and the effective confining pressure.

The CSL is described through the formulation proposed by Li [30], opportunely modified for unsaturated soils through the introduction of a bonding parameter (ξ) [33], which takes in account the effects of matric suction (related to capillary forces) and saturation degree. Analytical formulation for CSL is given by Eq. (5), where e_{CS} and p'_{CS} are the void ratio and the confining pressure at critical state in saturated condition, e_Γ is the void ratio at atmospheric pressure (p_{atm}) and λ is the slope of the CSL in $e\text{-}(p'/p_{atm})^{\xi c}$ plane. It is of paramount importance the definition of CSL for unsaturated state. Therefore, the model incorporate a bonding parameter ξ proposed by Gallipoli et al. [20] that measures the magnitude of the inter-particle bonding due to water menisci. It is defined as the product of two factors: (i) the saturation degree of air ($1\text{-}S_r$), which represents the number of water menisci per unit volume of solid fraction, and a (ii) function of suction $f(s)$, which accounts for the effect of matric suction on the stabilising inter-particle force exerted by a single meniscus. Particularly, the function $f(s)$ varies monotonically between 1 and 1.5 for suction ranging from 0 to infinity; $f(s)$ depends on the size of spheres and on the value of the water surface tension. The MPZ use the function $g(\xi)$ (Eq. (6)) to link the values of the critical effective stress p' at saturation and at a given suction for a fixed void ratio (Eq. (5)). Therefore, the function g(ξ) define the dependence of CSL on matric suction.

The flow rule depends on void ratio and, therefore, on the state parameter [32,33]. Rowe [61] proposed that dilatancy ($d = \Delta\varepsilon_v/\Delta\varepsilon_s$, with $\varepsilon_v = \varepsilon_1 + \varepsilon_2 + \varepsilon_3$ volumetric strain, and $\varepsilon_s = 1/3(\varepsilon_1 - \varepsilon_3)\cdot(\varepsilon_1 - \varepsilon_2)$ deviatoric strain, where ε_1, ε_2 and ε_3 are the principal strains) depends on the stress ratio, while Li and Dafalias [29] showed that the stress ratio at which the behaviour changes from contractive to dilative

is not constant and depends on void ratio. In other words, the dilatancy for a given stress ratio could be of different signs for dense or loose material. The dilatancy equation (Eq. (8)) used in the MPZ model is that proposed by Li and Dafalias [29] where M_g is the slope of the Critical State Line in the q-p' plane, η is the ratio between the mean effective stress p' and the deviatoric stress q, while d_0 and m are model parameters. The parameter M_f (Eq. (9)) is a function of the model constants h_1 and h_2, the parameter M_g and the ratio between the current void ratio e_0 and the void ratio at critical state e_{crit}.

The plastic modulus (H_L) is a function of the state parameter and the confining pressures (Eq. (11)), where H_0 and β'_0 are model parameters. The function H_{DM} incorporates the material memory into the plastic modulus equation. The dependence of the plastic modulus from the state parameter allows considering the dependency of both peak stress and after-peak behaviour on initial condition, and improves also the capacity of the model to predict the plastic deformation of specimens with different relative density through a unique set of model parameters.

The Soil Water Retention Curve (SWRC) is described through a modified version (Eq. (12)) of the equation proposed by Fredlund and Xing [18], where matric suction is replaced by the normalized suction (s^*) that accounts for the void ratio dependency (Eq. (13)) through another model parameter named Ω. Finally, the elastic constants (Eqs. (14) and (15)) are assumed depending on confining pressure and the void ratio as proposed by Richart et al. [43], where G_{es0} and K_{ev0} are model constants, corresponding to shear stiffness and volumetric stiffness, respectively.

Consideration of time dependency of the material behaviour is not taking into account in this version of MPZ model. All the equations of the model are listed below.

$$\frac{e_\Gamma - e_{CS}}{\lambda} = \left(\frac{p'_{CS}}{p_{atm}}\right)^{\zeta_c} \tag{5}$$

$$g(\xi) = a[\exp(b\xi) - 1] \tag{6}$$

$$p'_{CSunsat} = p'_{CSsat} \cdot \exp[g(\xi)] \tag{7}$$

$$d = \frac{d_0}{M_g}(M_g \exp^{m\psi} - \eta) \tag{8}$$

$$M_f = M_g\left[h_1 - h_2\left(\frac{e_0}{e_{crit}}\right)^{\beta}\right] \tag{9}$$

$$\beta_v = \frac{1}{\psi_p} ln\left(\frac{M_g}{\eta_p}\right) \tag{10}$$

$$H_L = H'_0 \exp(-\beta'_0 \psi_q) \cdot \sqrt{p' \cdot p'_{atm}} \cdot H_{DM} \tag{11}$$

$$S_r = S_{r0} + (1 - S_{r0})\left\{\ln\left[\exp(1) + \left(\frac{s^*}{a_w \cdot p_{atm}}\right)^n\right]\right\}^{-m} \tag{12}$$

$$s^* = e^{\Omega} \cdot s \tag{13}$$

$$G_{es} = G_{es0} \cdot \frac{(2.97 - e)^2}{(1 + e)} \cdot \sqrt{p' \cdot p_{atm}} \tag{14}$$

$$K_{ev} = K_{ev0} \cdot \frac{(2.97 - e)^2}{(1 + e)} \cdot \sqrt{p' \cdot p_{0\,atm}} \tag{15}$$

The MPZ model is quite comprehensive but requires the calibration of several constitutive parameters for: (i) saturated condition, such as elastic moduli (G_{es0} and K_{ev0}), Critical State parameters (M_g, e_{crit}, λ and ζ_c), those for plastic flow (h_1, h_2, d_0 and m), and for plastic modulus (H_0, β'_0, H_{v0}, and β_v), and (ii) unsaturated condition, such as bonding parameters (a, b and c), and those for SWRC (S_{r0}, Ω, $a_{w/d}$, $n_{w/d}$, $m_{w/d}$, and β_w). The large number of parameters is related to the complexity of the model. However, rainfall-induced wetting processes eventually combined to volumetric collapse and hydro-mechanical coupled soil mechanical response, demands for very general models, such as MPZ, which must necessarily be feed with many input parameters. In this sense, it is valuable that this paper proposes: (i) a procedure for a relatively simple (and standardized) model calibration, (ii) quantitative assessment of model performance. In the following sections, a systematic calibration procedure for volcanic soils is developed and the performance of MPZ model is evaluated through specific error functions.

4. Model calibration

Calibration and optimization of models are well-established topics in soil mechanics and geotechnical engineering. Many highly-specialized techniques have been proposed so far [27,28], among others). Recently, Cuomo et al. [13] and Calvello et al. [6] used a modified Gauss-Newton method with a weighted least-squares objective function for calibration of a rheological soil model, used for landslide propagation simulation. Another contribution based on a Bayesian data assimilation method was provided by Brezzi et al. [5]. On the other hand, Cuomo et al. [14], Cuomo et al. [15] applied a Species-based Quantum Particle Swarm Optimization (SQPSO) algorithm for calibration of a hypoplasticity model in the framework of a landslide triggering simulation. A recent review of optimization techniques widely used in geotechnical engineering is presented by Yin et al. [57]. However, the use of such advanced techniques was beyond the scope of this paper. Thus, a least squares algorithm was selected, and some equations of the constitute models were re-casted to be directly used for the calibration of the model parameters.

The elastic parameters (G_{eso} and K_{evo}, Eqs. (14) and (15) were calibrated based on the results of 6 triaxial tests, of which 3 for saturated and 3 for unsaturated specimens (Table 1). The tests on saturated specimens were performed in drained condition, and the tests on unsaturated specimens performed at different constant suction (10, 20 and 50 kPa). The shear modulus G_{eso} was found fitting by trial-and-error the initial slope of the q-ε_q plots (Fig. 4a and c), while the bulk modulus K_{evo} was adjusted fitting the initial slope of p'-ε_v curves (Fig. 4b and d). The estimates of G_{eso} and K_{evo} were searched at small deviatoric and volumetric strains (< 0.05) and it resulted $600\,\text{kPa} < G_{eso} < 2000\,\text{kPa}$ while $690\,\text{kPa} < K_{evo} < 3000\,\text{kPa}$ (Fig. 4c and d).

The parameter M_g (Eqs. (8) and (9)) was computed as the slope angle of the line interpolating with nil intercept the critical state points (derived from 3 drained and 3 undrained triaxial tests, and for suction from 10 to 50 kPa) in the q-p′ plane (Fig. 5a). The parameters of CLS (Eq. (5)) e_Γ, λ and ξ were calibrated based on the results of 8 CIU and 4 CID tests on saturated specimens, plotting the void ratio at critical state versus three different values of $(p'/p_{atm})^{\zeta c}$, where ζ_c was imposed equal to 0.6, 0.65, 0.7 and 0.8, respectively (Fig. 5b); between those value the best one was 0.6. Thus, the model parameters adopted for critical state were: $M_g = 1.55$, $e_\Gamma = 1.98$, $\lambda = 0.39$ and $\zeta_c = 0.6$.

The parameters (m, d_0) were evaluated through CID triaxial tests performed on saturated specimens and SCTX tests on unsaturated specimens at constant suction (Fig. 6 and Tables 1 and 2). The parameter m was calibrated through 6 CID tests and 2 SCTX tests at Critical State points where dilatancy (d) vanishes. Here, for $d = 0$ the Eq. (8) reads as $\eta_{CS} = M_g \cdot \exp(m \cdot \psi_{CS})$, where η_{CS} is the stress ratio and ψ_{CS} is the state parameter, both evaluated at Critical State, M_g is the slope of the Critical State Line in the q-p' plane, and m is the model parameter to be fitted. Thus, in Fig. 6a we refer to this exponential relationship, which can be used for different types of soils, as shown by Manzanal et al. [32], Manzanal et al. [33]. In the literature, different equations for dilatancy have been proposed. Linear equations were proposed by Manzari and Dafalias [35] and Gajo and Wood [19]. In the case of the MPZ model, an exponential equation similar to that proposed by Li and Dafalias [29] was assumed to capture the drained and undrained

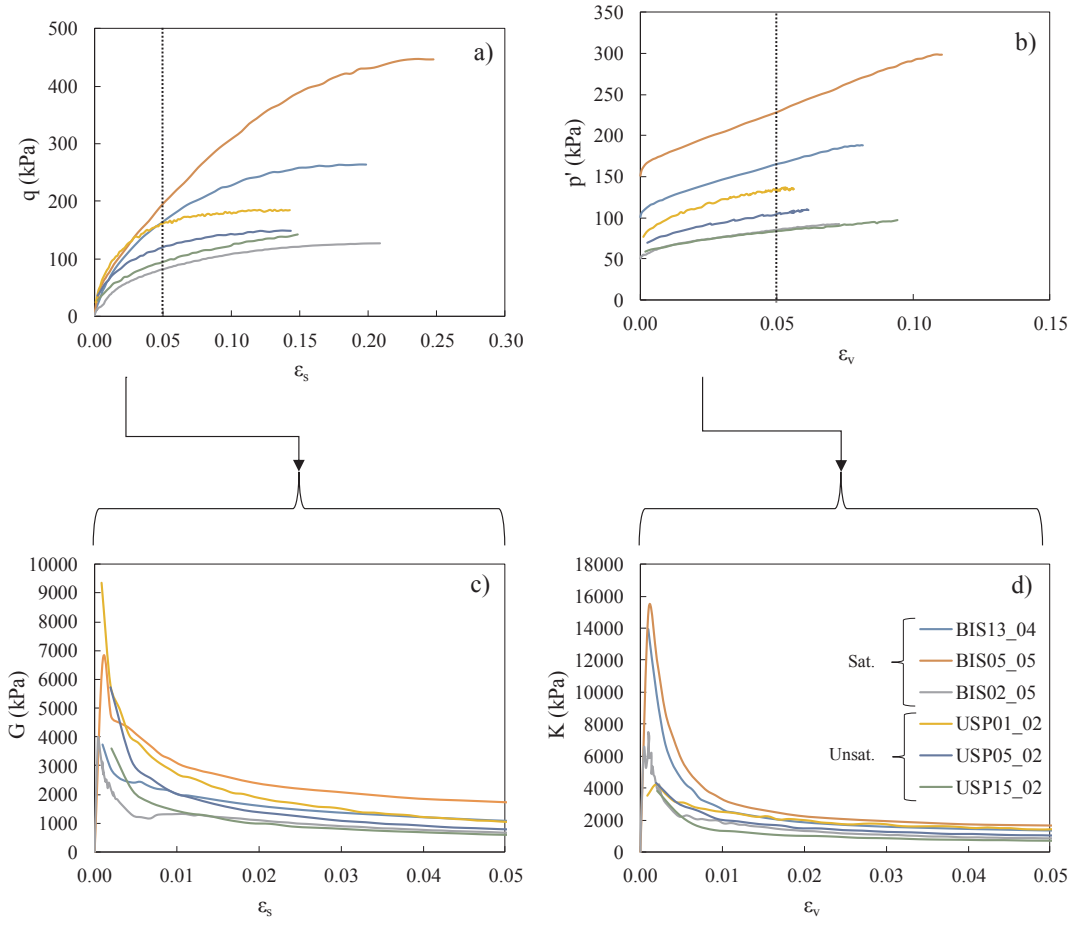

Fig. 4. Results of triaxial tests (a and b) and estimates of G_{es0} and K_{ev0} values for ε_s and ε_v < 0.05 (c and d).

behaviour for a wide range of confinement densities and pressures for different types of soil. In fact, for the pyroclastic soil considered in this paper, a linear relationship would be sufficient. However, we preferred to refer to the general Eq. (8), while not applying soil-specific relationships. In this way, the proposed procedure could be applied also to other types of soils. Doing so, the best estimate of m was 0.10 (Fig. 6a). On the other hand, the parameter d_0 was calibrated through the Least Squares Method, best-fitting two plots: (i) the measured dilatancy $d^{(exp)} = \Delta\varepsilon_v/\Delta\varepsilon_s$ versus the axial strain (ε_a), represented as dots in Fig. 6b, obtained from 3 CID triaxial tests on saturated specimens and 2 SCTX tests, and (ii) the values of dilatancy $d^{(mod)}$ modelled through Eq. (8) versus ε_a, represented by the red solid line in Fig. 6b. This calibration procedure relies on the hypothesis that, in the CID triaxial tests, elastic deformations are negligible, thus total strains are equal to the plastic ones. The estimated value of d_0 was 1.73 (Fig. 6b).

The plastic flow parameters h_1 and h_2 are function of initial void ratio and the void ratio at critical state (Fig. 7a). They were calibrated on the CID triaxial tests, assuming that M_f is related to relative density (D_r) according the relation $M_f/M_g = D_r$ [58]. The Eq. (9) was compared with the experimental value obtained through the relation $M_f/M_g = D_r$ (Fig. 7b). The results are quite satisfactory with $R^2 = 0.90$.

The parameters related to plastic modulus were calibrated through the results of triaxial and isotropic tests, in saturated and unsaturated conditions. The parameter β_v was calculated through Eq. (10) and the highest value of η of 8 CID triaxial tests on saturated specimens and 3 triaxial tests at constant suction (Fig. 8a). The constant H'_0 and H_{v0},

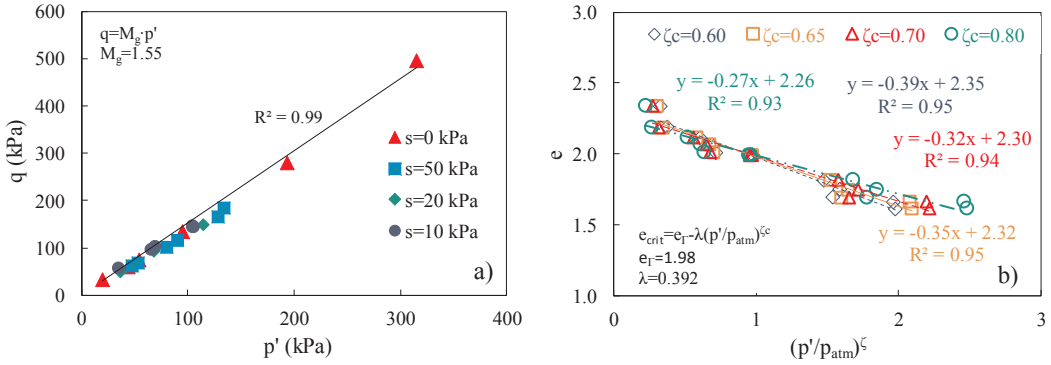

Fig. 5. Calibration of the critical state parameters in saturated conditions through drained and undrained triaxial tests: (a) calibration of the parameter M_g; (b) calibration of the parameters e_{atm}, λ, ζ_c.

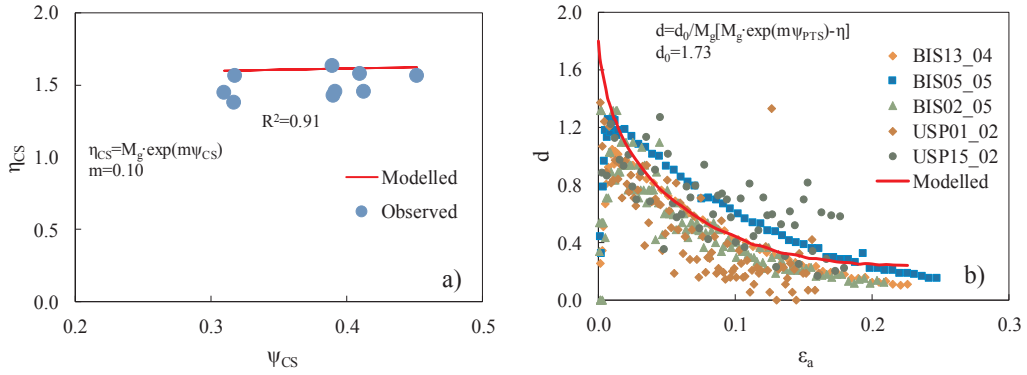

Fig. 6. Calibration of dilatancy-related parameters, such as "m" (a) and "d_0" (b).

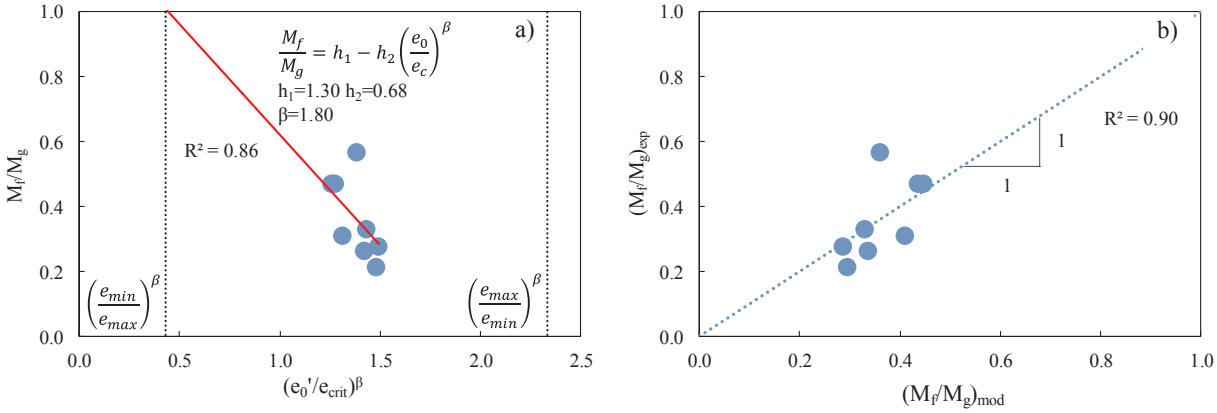

Fig. 7. (a) Calibration of the plastic flow parameters (h_1 and h_2); (b) comparison of experimental $(M_f/M_g)_{exp}$ and modelled $(M_f/M_g)_{mod}$ values.

which measures the distance between the CSL and ISL (Isotropic State Line) in saturated condition, were estimated assuming that H_{DM} is constant and equal to 1; this means that the specimens did not reach a η higher than the actual value. Doing so, and best-fitting the experimental plot of $H_L^{(exp)}$ and the values modelled through Eq. (11) $H_L^{(mod)}$ (Fig. 8b), it was found $H'_0 = 25.5$ and $H_{v0} = 2.3$.

The model parameters related to SWRC (S_{r0}, Ω, a_w, a_d, n_w, n_d, m_w, m_d) were evaluated through the Eq. (12) using the method proposed by Gallipoli et al. [20]. The Eqs. (12) and (13) were adopted to interpolate the experimental results of SWRC performed through suction-controlled oedometer, performed at different net vertical stress. As a choice of simplicity, one single SWRC was adopted both for drying and wetting paths (Fig. 9a), thus not using one of the potentialities of the model. The choice of one single SWRC is also suggested by the comparison of modelled ($S_{r,mod}$) and experimental ($S_{r,exp}$) of wetting and drying curves. The general fitting was satisfactory as $R^2 = 0.96$ (Fig. 9b).

The bonding parameters a and b were calibrated through triaxial tests at constant suction on unsaturated specimens (Fig. 10a). The parameters a and b were calibrated imposing the ratio $p'_{CSunsat}/p'_{CSsat}$ at a given void ratio equal to exp[g(ξ)] (Eq. (7)), which is a function of suction and degree of saturation (Eq. (6)). The general fitting was satisfactory as $R^2 = 0.82$ (Fig. 10a).

The parameter c is calibrated through isotropic triaxial tests carried out at constant suction 50 kPa (Fig. 10b). The experimental data are almost widespread and the general fit is $R^2 = 0.75$ (Fig. 10b).

The value of r_0 is equivalent to the OCR used in classical plasticity models and is taken equal to 1.44. The parameter related with accumulated deviatoric plastic strain is assumed equal $\beta_0 = 4.2$ and $\beta_1 = 0.20$ They have no real correlation with an specific test so they are still difficult to calibrate. For sake of simplicity, the values were selected based on previous literature [41,49,31]. The set of all the constitutive parameters is summarized in Table 4.

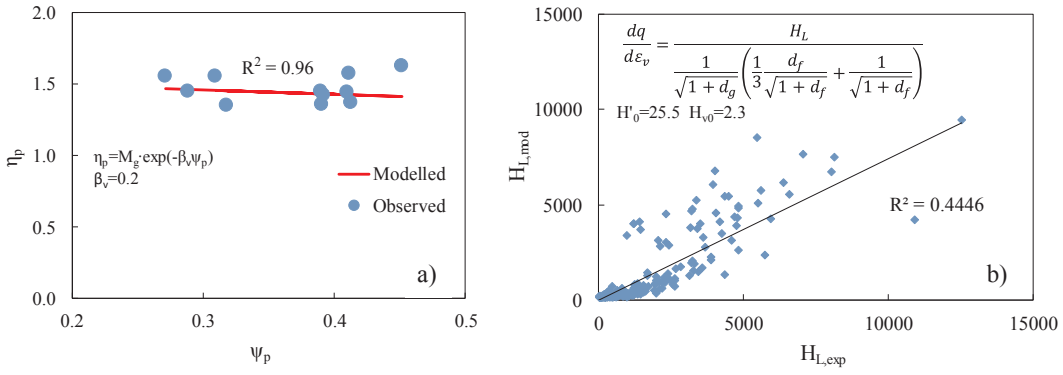

Fig. 8. (a) Calibration of plastic flow-related parameter "β_v"; (b) comparison of experimental ($H_{L,exp}$) and modelled ($H_{L,mod}$) values.

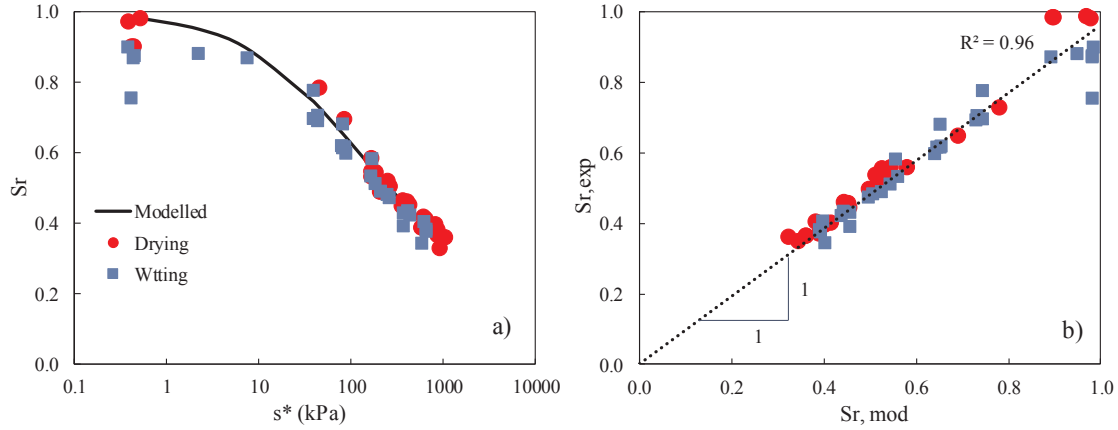

Fig. 9. (a) Calibration of model parameters for SWRC (Soil Water Retention Curve) as function of the normalized suction s^*, (b) comparison of experimental ($S_{r,exp}$) and modelled ($S_{r,mod}$) values.

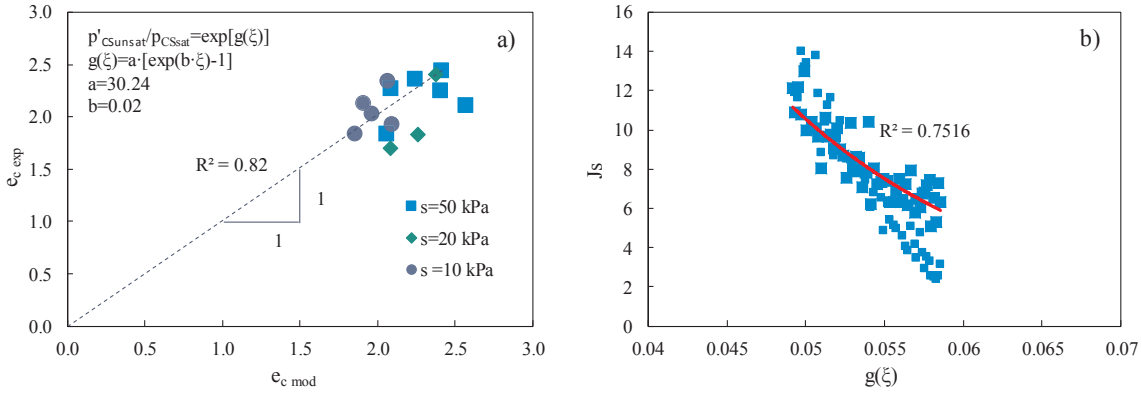

Fig. 10. (a) Calibration of the bonding parameters (*"a"and "b"*) through triaxial tests on unsaturated specimens performed at different suction. (b) Calibration of the bonding parameter "c" through isotropic tests on unsaturated specimens at suction 50 kPa.

Table 4
Constitutive parameters calibrated for the MPZ Model.

Elastic		Critical State			
G_{es0} (kPa)	K_{ev0} (kPa)	M_g	e_Γ	λ	ζ_c
1286	1746	1.55	1.98	0.39	0.6

Plastic flow				Plastic modulus				
h_1	h_2	d_0	m	H_0	β'_0	H_{v0}	β_v	r_0
1.30	0.68	1.73	0.10	25.50	4.2	2.3	0.20	1.44

Bonding			Water Retention Curve					
a	b	c	S_{r0}	Ω	a_w=a_d	n_w=n_d	m_w=m_d	β_w
30.24	0.02	0.7	0.354	1.61	0.48	0.69	1.21	2

5. Model performance

Calibration of the MPZ model was based on specific data extracted from the experimental results, while it is important assessing the real potential for the model to accurately reproduce the whole experimental results in terms of both stresses and strains for each test, and in different condition (saturated or unsaturated) or along different stress paths (e.g. in oedometer or triaxial devices). Aimed to provide an objective and quantitative estimate of the model performance, experimental and modelling results were compared referring to error functions, herein defined. Given n variables (stress or strain, each), e.g. named "F_i" with i = 1, …, n, the error function "$Err^{(Fi)}$" was defined with reference to the experimental value, $F_i^{(exp)}$, and the modelled one, $F_i^{(mod)}$, as follows:

$$Err^{(Fi)} = \frac{|F_i^{(exp)} - F_i^{(mod)}|}{|F_i^{(exp)}|} \quad (14)$$

In practice, the function "F_i" corresponded to: deviatoric stress (q), isotropic effective stress (p'), pore water pressure (u_w) or suction (s), axial strain (ε_a), volumetric strain (ε_v). It was expected that the error function may vary along one single test, and differently from one test to another, depending on type of test, confining stress, and specimen condition.

Three triaxial tests - performed in drained conditions on undisturbed saturated specimens (Table 1) were firstly referred in a narrow range of relative density ($0.27 < D_r < 0.39$). A large interval for the initial confining pressure (50 kPa $< p' <$ 150 kPa) was used to test the model performances.

The numerical results are provided in Fig. 11 in terms of q-ε_s, ε_v-ε_s, and e-p', where the experimental data are compared to the numerical results and the error functions are plotted. In q-ε_s plane, the performances were satisfactory in particular for the tests at confining pressure 50 kPa and 100 kPa. The error values were higher at low deviatoric strain (< 0.05) than at large deviatoric strain. The function $Err^{(q)}$ had the maximum value at deviatoric strain ranging between 0.001 and 0.003, while at deviatoric strain larger than 0.05 the error values were lower than 10% for the specimens at confining pressure 50 kPa and 10 kPa (BIS02_05 and BIS13_04) and lower than 23% for the specimen at confining pressure 150 kPa (Fig. 11a). The highest mean value of $Err^{(q)}$ was obtained for BIS08_04 (33.30%), while the lowest mean value was obtained for BIS02_05 (8.65%). The function $Err^{(ev)}$ had the same

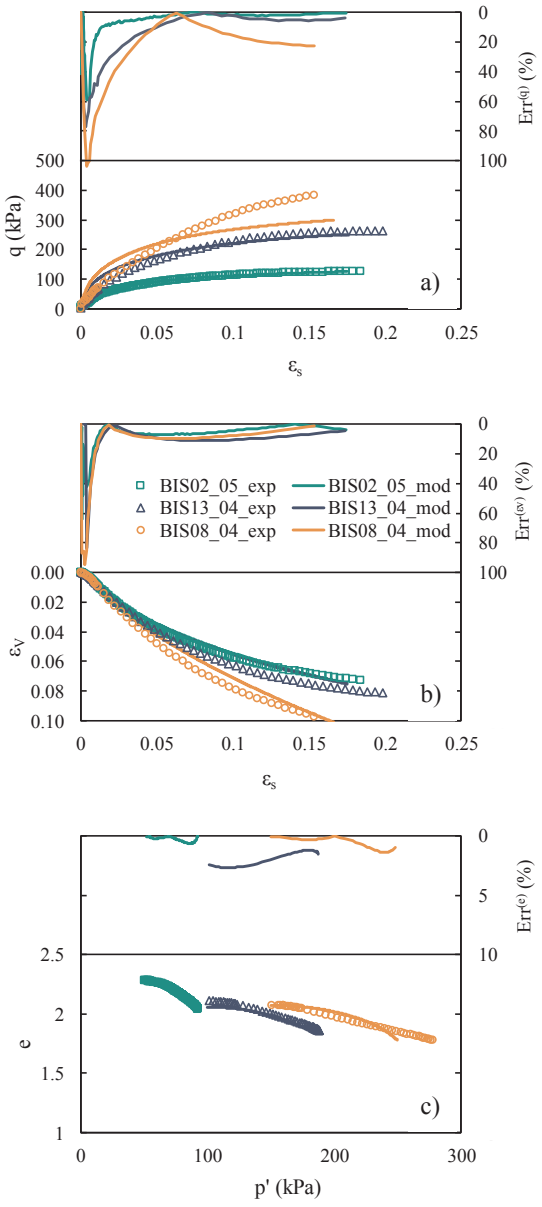

Fig. 11. Model Performance in Consolidated Isotropically Drained (CID) Triaxial tests on saturated soils: experimental (dots) versus modelling results (solid lines).

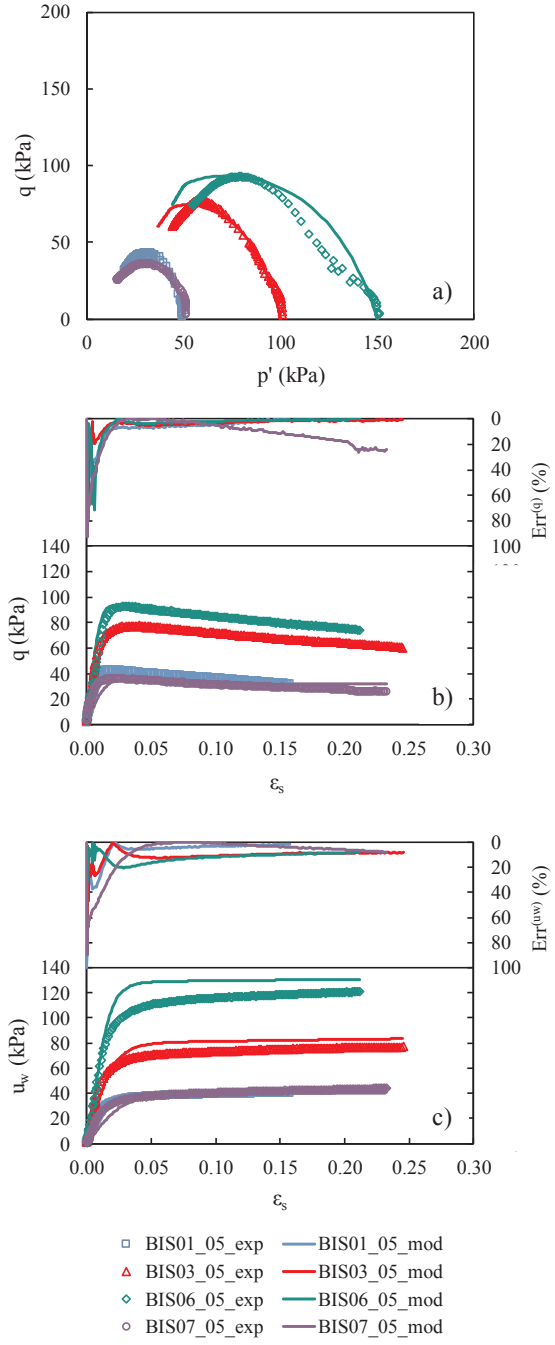

Fig. 12. Model Performance in Consolidated Isotropically Undrained (CIU) triaxial tests for saturated soils: experimental (squares) versus modelling results (solid lines).

trend of $Err^{(q)}$ with a maximum at lower deviatoric strain and values lower than 20% for deviatoric strain larger than 0.05 (Fig. 11b). The error in terms of volumetric strains was independent from confining pressure and the mean value of $Err^{(\varepsilon v)}$ varied between 14.11% and 21.21%. The function $Err^{(e)}$ was always less than 5% (Fig. 11c), the largest error was exhibited in the test BIS13_04 (2.66%).

The model was also adopted to simulate four triaxial tests in undrained conditions on saturated specimens. Three different confining pressures were selected (50 kPa, 100 kPa and 150 kPa). In q-p' plane, the best-fit was obtained for the tests BIS01_05, BIS03_05 and BIS07_05 (Fig. 11a). Both in q-ε_s and u-ε_s the errors are higher at low deviatoric strains (less than 0.01). On the other hand, at larger deviatoric strains the errors are lower than 20%. The best fit between experimental and numerical results was obtained for the tests BIS03_05, and BIS01_05 (Fig. 12b), the mean $Err^{(q)}$ were 7.88% and 11.32% respectively. $Err^{(q)}$ of the test BIS06_05 reached about 20% at deviatoric strain 0.21, which is the maximum error at large deviatoric strain (Fig. 12b). The mean error $Err^{(q)}$ was 12.23% for BIS06_05, while the highest value of $Err^{(q)}$ was found for BIS07_05 (12.66%). In u-ε_s plane, the best fit between experimental and numerical results was obtained for the tests at low confining pressure (p' = 50 kPa), BIS01_05 and BIS07_05 (Fig. 12c). The excess of pore water pressure was slightly overestimated by MPZ model for the tests BIS01_05 and BIS03_05 (Fig. 12c). The $Err^{(uw)}$ trend is almost equal for all tests: the mean value of $Err^{(uw)}$ varied between 6.92% (BIS06_05) and 11.76% (BIS07_05). The maximum $Err^{(uw)}$ corresponds to the test BIS07_05 (89.24%).

The model MPZ provides the possibility to individuate a unique set of constitutive parameters, which excellently simulates the behaviour of pyroclastic soils in (drained or undrained) triaxial tests, on specimens upon different p' and with different initial void ratio. This is because the dilatancy may change in the model in relation to the distance from the

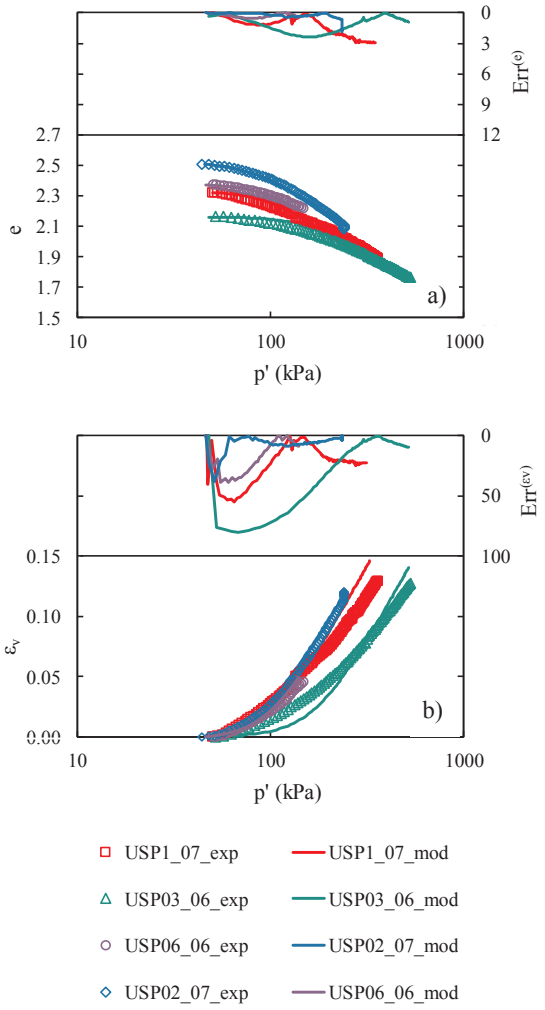

Fig. 13. Model Performance in Isotropic tests for unsaturated soils: experimental versus numerical results in the e-p' plane (a) and ε_v-p' (b).

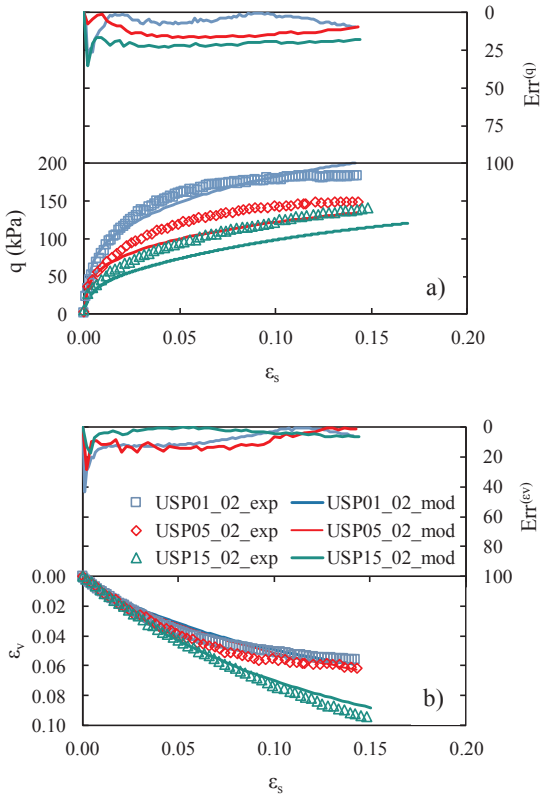

Fig. 14. Model Performance in Consolidated Isotropically suction-controlled triaxial tests for unsaturated soils: experimental (squares) versus modelling results (solid lines).

critical state line (i.e. proximity to failure).

The performances of MPZ model were also evaluated on unsaturated specimens. Isotropic compression tests and Consolidated Isotropically suction-controlled triaxial tests were simulated using a unique set of materials and constitutive parameters.

The model is able to reproduce the isotropic compression curve performed at suction 50 kPa (Fig. 13a and b). In e-p' plane, the results are great and the numerical results overlapped the experimental data. The best-fitting was obtained for USP06_06 and USP02_07, which have the function $Err^{(e)}$ always lower 2%, while USP01_07 and USP03_06 have $Err^{(e)}$ values lower than 3%. The functions $Err^{(e)}$ are significantly different each other, thus no trend can be distinguished, but the mean $Err^{(e)}$ for each test was in a narrow range, between 0.27% and 1.63%.

In p'-ε_v plane, the results are satisfactory even if the model overestimate the volumetric strain (Fig. 13b) at highest p'. The function $Err^{(\varepsilon v)}$ reached high values, such as 80.01% for USP03_06 and 53.02% for USP01_07. Each test reached the maximum of $Err^{(\varepsilon v)}$ at p' less than 100 kPa and the mean $Err^{(\varepsilon v)}$ varied between 5.32% (USP02_07) and 24.49% (USP03_06).

Three Consolidated Isotropically suction-controlled triaxial tests were used to evaluate the performances of the model. The tests were performed at suction 10 kPa, 20 kPa and 50 kPa (Table 2). The performances of MPZ model were evaluated both in q-ε_s and ε_v-ε_s through the function $Err^{(q)}$ and $Err^{(\varepsilon v)}$ (Fig. 14a and b). The best-fit in both planes was obtained for USP01_02 test, performed at suction 50 kPa, which has mean $Err^{(q)}$ = 5.42%, maximum $Err^{(q)}$ = 30.30%, mean $Err^{(\varepsilon v)}$ = 9.95% and maximum $Err^{(\varepsilon v)}$ = 43.41%. USP05_02 performed at suction 20 kPa exhibited the maximum value of mean $Err^{(q)}$ (9.92%), instead USP15_02 exhibited the maximum of mean $Err^{(\varepsilon v)}$ (17.06%). USP01_02 and USP15_02 reached maximum $Err^{(\varepsilon v)}$ at lower deformation, while $Err^{(\varepsilon v)}$ decreased slightly at large deviatoric strain (> 0.1), USP15_02 exhibited a different trend of $Err^{(\varepsilon v)}$. The function $Err^{(\varepsilon v)}$ was monotonic and its maximum value was higher than 20%.

The model performances were finally evaluated with reference to the collapse behaviour observed using different devices (standard oedometer, suction-controlled oedometer and suction-controlled triaxial).

Triaxial and oedometric wetting tests are simulated referring to the set of parameters already adopted to simulate Isotropic and triaxial tests at constant suction. Three net vertical stress (p-u_a = 100 kPa, low, 300 kPa, intermediate, and 500 kPa, high) were selected, while the initial suction value was 50 kPa for all the tests. The performances of the model were evaluated in ε_v-p' and ε_v-s (Fig. 15). The best numerical simulations of volumetric strain at collapse were obtained for wetting tests performed through standard oedometer (Fig. 15a), which have mean $Err^{(\varepsilon v)}$ lower than 3%. $Err^{(\varepsilon v)}$ at collapse varied from 1.36% and 14.02% for all types of wetting tests (Fig. 15b). The comparison among numerical and experimental results in ε_v-s plane is not useful to evaluate the performances about wetting tests performed through standard oedometer, because the specimens were saturated through flooding and only the volumetric strain at collapse can be measured (Fig. 15). Otherwise, the comparison of experimental and numerical results of wetting tests performed through suction-controlled triaxial and oedometer apparatus was the most useful to evaluate the performances of MPZ model. The mean $Err^{(\varepsilon v)}$ for wetting tests performed through suction-controlled triaxial and oedometer was higher than for other wetting tests (68.13% for ESA12_03). The $Err^{(\varepsilon v)}$ function reached its

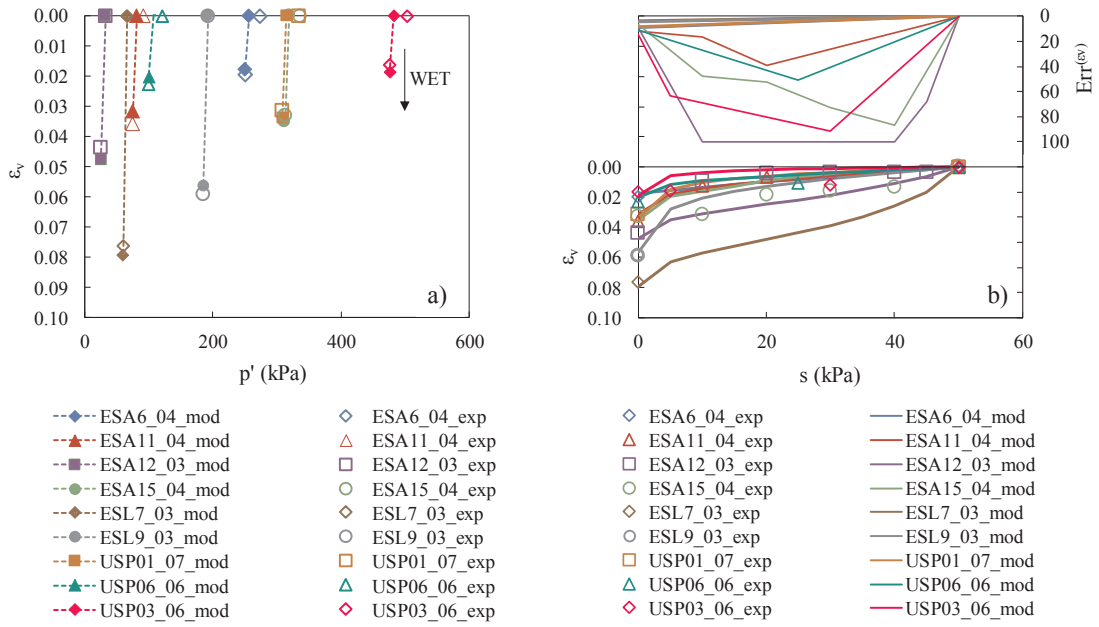

Fig. 15. Model Performance in Wetting tests performed in Suction-controlled Oedometer (ESA), Standard Oedometer (ESL) and Suction-controlled Triaxial (UPS): experimental versus numerical results in (ε_v-p') plane (a) and (ε_v -s) plane (b).

maximum at suction between 20 kPa and 40 kPa for wetting tests performed through suction-controlled oedometer and suction controlled triaxial (Fig. 15b). However, the whole amount of volumetric deformation at collapse of the unsaturated pyroclastic soil in the wetting tests was excellently simulated by the MPZ model, although the model exhibited high error along the suction reduction path, particularly for the tests performed through suction controlled oedometer.

6. Conclusions

Natural volcanic air-fall soils show peculiar features including static liquefaction in saturated condition for undrained shearing, and volumetric collapse in unsaturated conditions upon wetting. While there is a wide range of available constitutive models, the behaviour of such soils is still limitedly modelled because of the lack of extensive experimental laboratory tests on partially saturated soils.

The papers dealt with a natural volcanic silty soil of Southern Italy, widespread along steep slopes often involved in catastrophic landslides of the flow-type. Globally, this kind of soil poses major issues because once a slide has triggered, it may turn into a flow with high destructive potential. However, an overall characterization and modelling of such soil is challenging and not yet available in the literature.

A recent Generalized Plasticity Model selected as it is capable to adequately take into account: (i) soil porosity changes through a state parameter, namely the distance from critical state line in the plot of void ratio versus effective isotropic stress, (ii) bonding related to the matric suction normalized versus soil porosity, (iii) static liquefaction proneness.

The model was calibrated for 37 laboratory tests, either triaxial or oedometer, in saturated and unsaturated conditions, and the performance of the model was assessed comparing the experimental results versus those modelled. It was newly shown that the model – with one single set of constitutive parameters – is capable to well describe the soil mechanical response, in unsaturated and saturated conditions, tested in different laboratory devices along different stress paths. Those insights provide a sound theoretical framework for designing further laboratory tests, and improving the understanding of this complex natural soil. On the other hand, this advanced constitutive model can be a practical tool once implemented in a numerical code for the resolution of relevant boundary value problems such landslides of the flow-type.

As limitation of the present work, it is worth noting that a number of highly specialized optimization techniques were proposed, and applied to different kind of soil models, with application also to landslide analysis. The use of sophisticated optimization techniques was beyond the scope of this paper. Thus, a least squares algorithm was selected, and some equations of the used constitute model were re-casted to be directly used for the calibration of the model parameters. Future research could allow the application of optimization algorithms with the scope to achieve the minimum difference between the observations and the results of the modelling.

References

[1] Alonso EE, Gens A, Josa A. Constitutive model for partially saturated soils. Géotechnique 1990;40(3):405–30.
[2] Bilotta E, Cascini L, Foresta V, Sorbino G. Geotechnical characterisation of pyroclastic soils involved in huge flowslides. Geotech Geol Eng 2005;23(4):365–402.
[3] Bilotta E, Foresta V, Migliaro G. The influence of suction on stiffness, viscosity and collapse of some volcanic ashy soils. In: Toll, et al., editors, Unsaturated soils: advances in geo-engineering; 2008. p. 349–54, ISBN 978-0-415-47692-8.
[4] Bishop AW. The principle of effective stress. Tek Ukeblas 1959;39:859–63.
[5] Brezzi L, Bossi G, Gabrieli F, Marcato G, Pastor M, Cola S. A new data assimilation procedure to develop a debris flow run-out model. Landslides 2016;13(5):1083–96.
[6] Calvello M, Cuomo S, Ghasemi P. The role of observations in the inverse analysis of landslide propagation. Comput Geotech 2017;92:11–21.
[7] Cascini L, Cuomo S, Pastor M, Sacco C. Modelling the post-failure stage of rainfall-induced landslides of the flow-type. Can Geotech J 2013;50(9):924–34.
[8] Cascini L, Cuomo S, Guida D. Typical source areas of May 1998 flow-like mass movements in the Campania region, Southern Italy. Eng Geol 2008;96:107–25.
[9] Cascini L, Cuomo S, Pastor M, Sorbino G. Modelling of rainfall-induced shallow landslides of the flow-type. ASCE's J Geotech Geoenviron Eng 2010;1:85–98.
[10] Chiu CF, Ng CWW, Shen CK. Collapse behaviour of loosely compacted virgin and non-virgin fills in Hong Kong. In: Proc. 2nd int. conf. unsaturated soils, vol. 1; 1998. p. 25–30.
[11] Chu J, Leroueil S, Leong WK. Unstable behaviour of sand and its implications for slope instability. Can Geotech J 2003;40:873–85.
[12] Cuomo S. Geomechanical modelling of triggering mechanisms for flow-like mass movements in pyroclastic soils [Ph.D. Thesis Dissertation]. University of Salerno; 2006. p. 274.
[13] Cuomo S, Calvello M, Villari V. Inverse analysis for rheology calibration in SPH analysis of landslide run-out. Engineering geology for society and territory, vol. 2. Cham: Springer; 2015. p. 1635–9.
[14] Cuomo S, Ghasemi P, Calvello M, Hosseinezhad V. Hypoplasticity model and inverse analysis for simulation of triaxial tests. In: Proc. of UNSAT conference, August 2018, Hong Kong (China); 2018, in press.
[15] Cuomo S, Ghasemi P, Martinelli M, Calvello M. Simulation of liquefaction and retrogressive slope failure in loose coarse-grained material. ASCE Geomech J 2018.

submitted for publication.
[16] Cuomo S, Moscariello M, Salager S. Grain scale mechanisms for capillary collapse in a loose unsaturated pyroclastic soil. In: E3S Web of conferences, EDP Sciences, vol. 9; 2016. p. 06002.
[17] Fernandez Merodo JA, Pastor M, Mira P, Tonni L, Herreros MI, Gonzalez E, et al. Modelling of diffuse failure mechanisms of catastrophic landslides. Comput Methods Appl Mech Eng 2004;193:2911–39.
[18] Fredlund DG, Xing A. Equations for the soil-water characteristic curve. Can Geotech J 1994;31(4):521–32.
[19] Gajo A, Wood M. Severn-trent sand: a kinematic-hardening constitutive model: the q–p formulation. Géotechnique 1999;49(5):595–614.
[20] Gallipoli D, Gens A, Sharma R, Vaunat J. An elasto-plastic model for unsaturated soil incorporating the effects of suction and degree of saturation on mechanical behaviour. Géotechnique 2003;53(1):123–36.
[21] Hill R. A variational principle of maximum plastic work in classical plasticity. Quart J Mech Appl Math 1948;1(1):18–28.
[22] Jennings JE, Knight K. The additional settlement of foundations due to a collapse of structure of sandy subsoils on wetting. In: Proceedings; 1957. p. 316–19.
[23] Kato S, Kawai K. Deformation characteristics of a compacted clay in collapse under isotropic and triaxial stress state. Soils Found 2000;40(5):75–90.
[24] Lade PV. Static instability and liquefaction of loose fine sandy slopes. J Geotech Eng ASCE 1992;118(1):51–71.
[25] Lancellotta R, Di Prisco C, Costanzo D, Foti S, Sorbino G, Buscarnera G, et al. Caratterizzazione e modellazione geotecnica. In: Criteri di zona-zione della suscettibilità e della pericolosità da frane innescate da eventi estremi (piogge e sisma). Leonardo Cascini. Composervice srl, Padova; 2012. p. 266–319.
[26] Lawton EC, Fragaszy RJ, Hardcastle JH. Stress ratio effects on collapse of compacted clayey sand. J Geotech Eng 1991;117(5):714–30.
[27] Le TM, Fatahi B. Trust-region reflective optimisation to obtain soil visco-plastic properties. Eng Comput 2016;33(2):410–42.
[28] Le TM, Fatahi B, Khabbaz H. Numerical optimisation to obtain elastic viscoplastic model parameters for soft clay. Int J Plast 2015;65:1–21.
[29] Li XS, Dafalias YF. Dilatancy for cohesionless soils. Géotechnique 2000;50(4):449–60.
[30] Li XS. Modeling of dilative shear failure. J Geotech Geoenviron Eng 1997;123(7):609–16.
[31] Manzanal D. Constitutive model based on generalized plasticity incorporating state parameter for saturated and unsaturated sand (Spanish) [Ph.D. Thesis]. School of Civil Engineering, Polytechnic University of Madrid; 2008. p. 334.
[32] Manzanal D, Merodo JA, Pastor M. Generalized plasticity state parameter-based model for saturated and un-saturated soils. Part I: Saturated state. Int J Numer Anal Methods Geomech 2011;35(12):1347–62.
[33] Manzanal D, Pastor M, Merodo JA. Generalized plasticity state parameter-based model for saturated and unsaturated soils. Part II: Unsaturated soil modeling. Int J Numer Anal Meth Geomech 2011;35(18):1899–917.
[34] Manzanal D, Pastor M, Fernández Merodo JA, Mira P, Martín Stickle M, Yagüe A, et al. Generalized plasticity modelling of geomaterials: the rol of dilatancy. In: Schrefler B, Sanavia L, Collin F, editors, Coupled and multiphysics phenomena: ALERT Doctoral School 2015; 2015. ISBN 978-2-9542517-6-9.
[35] Manzari MT, Dafalias YF. A critical state two-surface plasticity model for sands. Geotechnique 1997;47(2):255–72.
[36] Migliaro G. Il legame costitutivo dei terreni piroclastici per la modellazione di scavi in ambiente urbanizzato ed in-fluenza della parziale saturazione [PhD. Thesis]. Italy: Università degli studi di Salerno; 2008. p. 305p.
[37] Mira P. Modeling of foundations of marine structures. Technical report of the Geotechnical Laboratory of CEDEX for Puertos del Estado. Spain. (Spanish); 2014. p. 270. December 2014.
[38] Mira P, Fernadez Merodo JA, Pastor M, Manzanal D, Stickle M, Yagüe A. A methodology for the study of foundations for marine structures. In: ALET geomaterials workshop. Poster session. Aussois, France; 2016. p. 55–6, ISBN 978-2-9542517-7-6.
[39] Olivares L, Damiano E. Postfailure mechanics of landslides: laboratory investigation of flowslides in pyroclastic soils. J Geotech Geoenviron Eng ASCE 2007;1331:51–62.
[40] Pastor M, Manzanal D, Merodo JA, Mira P, Blanc T, Drempetic V, et al. From solid to fluidized soils: diffuse failure mechanisms in geostructures with applications to fast catastrophic landslides. Granular Matter 2009;12(3):211–328.
[41] Pastor M, Zienkiewicz OC, Chan AHC. Generalized plasticity and the modelling of soil behaviour. Int J Numer Anal Meth Geomech 1990;14(3):151–90.
[42] Pereira JH, Fredlund DG. Volume change behavior of collapsible compacted gneiss soil. J Geotech Geoenviron Eng 2000;126(10):907–16.
[43] Richart FE, Hall JR, Woods RD. Vibrations of soils and foundations. Prentice-Hall; 1970.
[44] Roscoe KH. An apparatus for the application of simple shear to soil samples. In: Proceedings of 3rd international conference on soil mech. and found. eng., Zurich, vol. 1; 1953. p. 186–91.
[45] Sorbino G, Migliaro G, Foresta V. Laboratory investigations on static liquefaction potential of pyroclastic soils involved in rainfall-induced landslides of the flow-type. In: Proceedings of the 5th international conference on unsaturated soils, London, vol. 1; 2011. p. 375–80.
[46] Sorbino G, Nicotera MV. Unsaturated soil mechanics in rainfall-induced flow landslides. Eng Geol 2013;165:105–32.
[47] Suriol J, Gens A, Alonso EE. Behaviour of compacted soils in suction controlled oedometer; 1998.
[48] Tamagnini R, Pastor M. A thermodynamically based model for unsaturated soils: a new framework for generalized plasticity. In: Proceeding of the 2nd international workshop on unsaturated soils, Mancuso Ed. Naples, Italy; 2004. p. 1–14.
[49] Tonni L, Gottardi G, Simonini P, Pastor M, Mira P. Use of Generalized Plasticity to describe the behaviour of a wide class of non-active natural soils. In: 3rd international symposium on deformation characteristics of geomaterials; 2003. p. 1145–53.
[50] Van Asch ThWJ, Malet JP, van Beek LPH. Influence of landslide geometry and kinematic deformation to describe the liquefaction of landslides: some theoretical considerations. Eng Geol 2006;88:59–69.
[51] Van Genuchten MT. A close form equation predicting the hydraulic conductivity of unsaturated soil. Soil Sci Soc Am J 1980;44:892–8.
[52] Vilar OM, Davies GI. Collapse behavior analysis of a clayey sand using different testing procedures. Unsaturated Soils 2002;2:571–6.
[53] Wanatowski D, Chu J. Static liquefaction of sand in plane-strain. Can Geotech J 2007;44(3):299–313.
[54] Wanatowski D, Chu J. Factors affecting pre-failure instability of sand under plane-strain Conditions. Geotechnique 2012;62(2):121–35.
[55] Wheeler SJ, Sivakumar V. An elasto-plastic critical state framework for unsaturated soil. Géotechnique 1995;45(1):35–53.
[56] Yamamuro JA, Lade PJ. Steady-state concepts and static liquefaction of silty sands. ASCE J Geotech Geoenviron Eng 1998;1249:868–78.
[57] Yin ZY, Jin YF, Shen SL, Huang HW. An efficient optimization method for identifying parameters of soft structured clay by an enhanced genetic algorithm and elastic–viscoplastic model. Acta Geotech 2017;12(4):849–67.
[58] Zienkiewicz OC, Chan AHC, Pastor M, Shrefler BA, Shiomi T. Computational geomechanics. J. Wiley and Sons; 1999.
[59] Barden L, McGown A, Collins K. The collapse mechanism in partly saturated soil. Eng Geol 1973;7(1):49–60.
[60] Cuomo S, Pastor M, Cascini L, Castorino GC. Interplay of rheology and entrainment in debris avalanches: a numerical study. Can Geotech J 2014;51(11):1318–30.
[61] Rowe PW. The stress-dilatancy relation for static equilibrium of an assembly of particles in contact. Proc R Soc Lond - The Royal Society 1962;269(1339):500–27.